



This is a repository copy of *Identification of the hydrate gel phases present in phosphate-modified calcium aluminate binders.*

White Rose Research Online URL for this paper:
<http://eprints.whiterose.ac.uk/86430/>

Version: Accepted Version

Article:

Chavda, M.A., Bernal, S.A., Apperley, D.C. et al. (2 more authors) (2015) Identification of the hydrate gel phases present in phosphate-modified calcium aluminate binders. *Cement and Concrete Research*, 70. 21 - 28. ISSN 0008-8846

<https://doi.org/10.1016/j.cemconres.2015.01.007>

Reuse

Unless indicated otherwise, fulltext items are protected by copyright with all rights reserved. The copyright exception in section 29 of the Copyright, Designs and Patents Act 1988 allows the making of a single copy solely for the purpose of non-commercial research or private study within the limits of fair dealing. The publisher or other rights-holder may allow further reproduction and re-use of this version - refer to the White Rose Research Online record for this item. Where records identify the publisher as the copyright holder, users can verify any specific terms of use on the publisher's website.

Takedown

If you consider content in White Rose Research Online to be in breach of UK law, please notify us by emailing eprints@whiterose.ac.uk including the URL of the record and the reason for the withdrawal request.



eprints@whiterose.ac.uk
<https://eprints.whiterose.ac.uk/>

Identification of the hydrate gel phases present in phosphate-modified calcium aluminate binders

Mehul A. Chavda¹, Susan A. Bernal¹, David C. Apperley², Hajime Kinoshita¹ and John L. Provis^{1*}

¹*Department of Materials Science and Engineering, The University of Sheffield, Sheffield S1 3JD, United Kingdom*

²*Solid-State NMR Group, Department of Chemistry, Durham University, Durham DH1 3LE, United Kingdom*

* *To whom correspondence should be addressed. Email j.provis@sheffield.ac.uk, phone +44 114 222 5490, fax +44 114 222 5493*

Abstract

The conversion of hexagonal calcium aluminate hydrates to cubic phases in hydrated calcium aluminate cements (CAC) can involve undesirable porosity changes and loss of strength. Modification of CAC by phosphate addition avoids conversion, by altering the nature of the reaction products, yielding a stable amorphous gel instead of the usual crystalline hydrate products. Here, details of the environments of aluminium and phosphorus in this gel were elucidated using solid-state NMR and complementary techniques. Aluminium is identified in both octahedral and tetrahedral coordination states, and phosphorus is present in hydrous environments with varying, but mostly low, degrees of crosslinking. A ³¹P/²⁷Al rotational echo adiabatic passage double resonance (REAPDOR) experiment showed the existence of aluminium–phosphorus interactions, confirming the formation of a hydrated calcium aluminophosphate gel as a key component of the binding phase. This resolves previous disagreements in the literature regarding the nature of the disordered products forming in this system.

Keywords: calcium aluminate cement; amorphous material; CP/MAS NMR; spectroscopy

1. Introduction

Calcium aluminate cements (CAC) are well known for their rapid hardening, early strength development, resistance to chemical attack [1], and low pore solution pH relative to Portland cement [2]. These properties have made them suitable for use in several key applications [3], including as a biomaterial for bone and dental repairs [4], refractory concretes [5,6], specialised mortars for structural applications [1], carbonation resistant geothermal well applications [7], and more recently immobilisation of metallic radioactive wastes [8-11] and toxic metal solutions [12].

During the hydration of monocalcium aluminate (CaAl_2O_4 , abbreviated CA^*), which is the main reactive phase within CAC, the precipitation of a poorly crystalline gel phase [1], and hexagonal and cubic calcium aluminate hydrate phases, have been observed [5]. Depending on the duration and temperature of curing, the metastable hexagonal phases (CAH_{10} and C_2AH_8) undergo a conversion process whereby they dissolve and re-precipitate as the stable cubic hydrogarnet (C_3AH_6), along with gibbsite and/or disordered aluminium hydroxide (AH_3). As a consequence of the differences in densities between the metastable and stable hydrate phases, this conversion can result in a significant loss of solid volume fraction within the hardened material, leading to a dramatic reduction in the loading capacity, and sometimes loss of mechanical integrity of the monolith [1]. Conversion is one of the main limiting factors of the widespread use of these

* This paper uses standard cement chemistry abbreviations, where CaO is represented as C; Al_2O_3 as A; SiO_2 as S; H_2O as H; P_2O_5 as P. Structural formulae for non-stoichiometric products are written in hyphenated form; i.e., C-A-H represents a non-stoichiometric (and structurally disordered) calcium aluminate hydrate, and analogously for silicate- and phosphate-containing products.

materials in construction; there have been several disastrous structural failures of CAC concretes in the past, which have led to prohibition of the use of CAC in structural elements in many countries [13].

Modification of CACs with the goal of avoiding the conversion of hexagonal to cubic hydrates, through the direct precipitation of stable hydrates, has thus been the focus of a number of studies over the past decades. Chemical modification of CAC has been conducted using highly alkaline solutions, including sodium hydroxide and sodium silicates [14] favouring the direct precipitation of C_3AH_6 or Si-substituted katoite as main reaction products respectively, hence avoiding the porosity development associated with the conversion of the intermediate metastable phases. Inclusion of supplementary siliceous cementitious materials (silica fume [15,16], fly ash [15,17], blast furnace slag [18]) has also been demonstrated to be an effective pathway to limit deleterious conversion, through promoting the formation of secondary products such as strätlingite (C_2ASH_8) and calcium silicate hydrate (C-S-H).

The addition of phosphate compounds to CAC [8,19-22] has been shown to be an effective route to avoid the conventional hydration of the CAC system and increase both the loading capacity and flexural strength, as it modifies the phase assemblage hydrated CAC and favours the precipitation of a poorly crystalline binder phase; however, the mechanism of reaction and chemistry of the reaction products forming in these systems are not yet well understood. Early studies conducted by Sugama et al. [21] suggested that the mechanism of reaction in ammonium phosphate-modified CAC takes place via an acid-base reaction, between the acidic phosphate solution and the basic calcium aluminate cement. This system has been reported to favour the

precipitation of ammonium calcium phosphates, either $(\text{NH}_4)_2\text{Ca}(\text{P}_2\text{O}_7)\cdot x\text{H}_2\text{O}$ or $\text{NH}_4\text{CaPO}_4\cdot x\text{H}_2\text{O}$ [19,21,23].

In the case of CAC blended with sodium monophosphate (NaH_2PO_4) and sodium polyphosphate ($(\text{NaPO}_3)_n$), the phase identification is still under discussion: formation of a sodium calcium orthophosphate hydrate ($\text{NaCaPO}_4\cdot x\text{H}_2\text{O}$) and alumina gel was originally proposed [20], while later work suggested instead the formation of a calcium hydrogen phosphate hydrate ($\text{Ca}(\text{HPO}_4)\cdot x\text{H}_2\text{O}$) and a hydrated alumina gel [24]. More recently, Swift et al. [8], investigating the effect of different phosphates with varying chain lengths on the hydration of CAC, concluded that the binder phase forming in this modified system was likely to be an amorphous calcium phosphate, along with alumina gel, similar to that proposed by Sugama et al. [24]. Conversely, Ma and Brown [22,25] reported the formation of a calcium aluminate phosphate hydrate (C-A-P-H) in their study of the effect of various sodium phosphates upon the hydration of CAC.

These clear discrepancies in the existing literature elucidate that there is not a good current understanding of the chemistry or mechanism of formation of the key binding phases in phosphate-modified CAC.

Solid-state nuclear magnetic resonance (NMR) spectroscopy has been used successfully in studying complex cement hydration processes due to its sensitivity to disordered as well as crystalline phases [26], including in the analysis of CACs [27-29]. Magic angle spinning (MAS) NMR spectroscopy has in particular been widely used to probe local environments of aluminium and silicon nuclei in cements. Nuclei such as ^{31}P have not been exploited to the same extent in

the context of cement chemistry, despite favourable NMR properties; notable investigations appear in the field of biocompatible dental cements [30,31] and the study of Portland cement [32]. For the phosphate-modified CAC systems studied here, ^{31}P is a key nucleus which has not previously been examined through the use of advanced NMR techniques.

Therefore, in this study we seek to better understand the phase chemistry in phosphate-modified calcium aluminate cements, specifically utilising solid-state NMR to characterise the poorly-understood amorphous binding phase and gain further insight into its formation. The phase assemblages formed in unmodified CAC, and CAC with sodium phosphate modification, are assessed using X-ray diffractometry, thermogravimetric analysis, and local environments are probed through solid state NMR spectroscopic techniques including ^{27}Al MAS, ^{31}P MAS, $^{31}\text{P}\{^1\text{H}\}$ CP/MAS, and $^{31}\text{P}/^{27}\text{Al}$ REAPDOR NMR.

2. Materials and methods

2.1. Materials

CAC supplied by Kerneos under the trade-name Secar 51 was used in this study as the primary precursor, and the oxide composition quantified by X-ray fluorescence analysis is shown in Table 1. Reagent grade sodium polyphosphate $((\text{NaPO}_3)_n)$, 97%, Acros Organics), comprising mainly long chains with a minor quantity of cyclic and cross linked phosphate [33], was also used.

Table 1. Oxide composition of Secar 51 from X-ray fluorescence analysis

| Raw Material | Chemical constituents (wt.% as oxide) | | | | | | | |
|-----------------|---------------------------------------|-------|------------------|--------------------------------|------------------|------|-----------------|--------------------------------------|
| | Al ₂ O ₃ | CaO | SiO ₂ | Fe ₂ O ₃ | TiO ₂ | MgO | SO ₃ | K ₂ O + Na ₂ O |
| Secar 51 | 50.77 | 38.39 | 4.83 | 1.82 | 2.04 | 0.40 | 0.24 | 0.63 |

2.2. Sample synthesis and testing procedures

Cement pastes were formulated with a water to cement ratio of 0.35, and a sodium polyphosphate to cement ratio of 0.4, defined on a mass basis. In addition, neat CAC pastes with the same water to cement ratio were prepared. The phosphate content was selected based on previous work [34] where this ratio of 0.4 was shown to hinder crystallisation of conventional CAC hydrates which are prone to conversion. Prior to the preparation of the paste, the solid sodium polyphosphate was mixed with distilled water on a roller mixer for 24 h at room temperature to ensure complete dissolution. The phosphate solutions were then added to the CAC clinker and hand mixed for 30 s, followed by 120 s of high shear mixing with a Silverson L4RT mixer at 2500 rpm. Samples were cast in centrifuge tubes, sealed and kept at a temperature of 20°C and 100% relative humidity for 7, 180 and 360 days.

Compressive strength measurements were carried out on a Zwick Roell testing instrument using demoulded samples and tested after the required curing period. Cylindrical samples were cut to an aspect ratio of 2 and a diameter of 14 mm, and tested to failure. Compressive strength was calculated as the force per unit area at the maximum load applied to the sample. Specimens were tested in triplicate, and specimen ends were polished to give flat faces perpendicular to the axis of the cylinders.

For study by other analytical techniques, hydration reactions were arrested by demoulding, crushing the samples to sub-cm³ sized pieces, and immersing in acetone. Samples were removed from the acetone after 24 h and dried at room temperature under atmospheric conditions (21°C), followed by storage in a vacuum desiccator until analysis. Samples were finely ground to less than 63 µm and then subjected to the following analyses:

- X-ray diffractograms were obtained using a Siemens D5000 diffractometer with a copper source, scanning in the 2θ range 5°-55° with a step size of 0.02° and at a rate of 1°/min.
- Thermogravimetric analysis was performed on a PerkinElmer Pyris 1 instrument, in an alumina crucible, heating from room temperature to 1000°C at a rate of 10°C/min, under a flowing nitrogen atmosphere.
- All NMR experiments were performed on a Varian VNMRS 400 spectrometer (9.4 T), using a CP/MAS probe with 4 mm o.d. zirconia (PSZ) rotors, and pulse sequences as shown in Figure 1.

A. ²⁷Al MAS NMR spectra were collected at 104.199 MHz and spinning speed 14.0 kHz (without proton decoupling), using a pulse delay of 0.2 s, a pulse width of 1.0 µs and an acquisition time of 10 ms, for 10,000 repetitions (Figure 1A). The chemical shifts were referenced to an external sample of 1.0 M aqueous solution of AlCl₃·6H₂O.

B. ³¹P MAS and CPMAS spectra were collected at 161.87 MHz with a spinning speed of 12.0 kHz and two pulse phase modulation (TPPM) decoupling at a nutation rate of 87 kHz (Figure 1B). MAS spectra were acquired using a 90° pulse of duration 3.8 µs,

a pulse delay of 60 s, an acquisition time of 30 ms, for 30 to 40 repetitions. $^{31}\text{P}\{^1\text{H}\}$

CP/MAS spectra were collected with a pulse delay of 30 s, a contact time of 1 ms and an acquisition time of 30 ms. The chemical shifts were referenced to an external sample of 85% H_3PO_4 .

C. $^{31}\text{P}/^{27}\text{Al}$ REAPDOR spectra were acquired at a spin rate of 10 kHz with a 60 s recycle delay, according to the pulse sequence shown in Figure 1C.

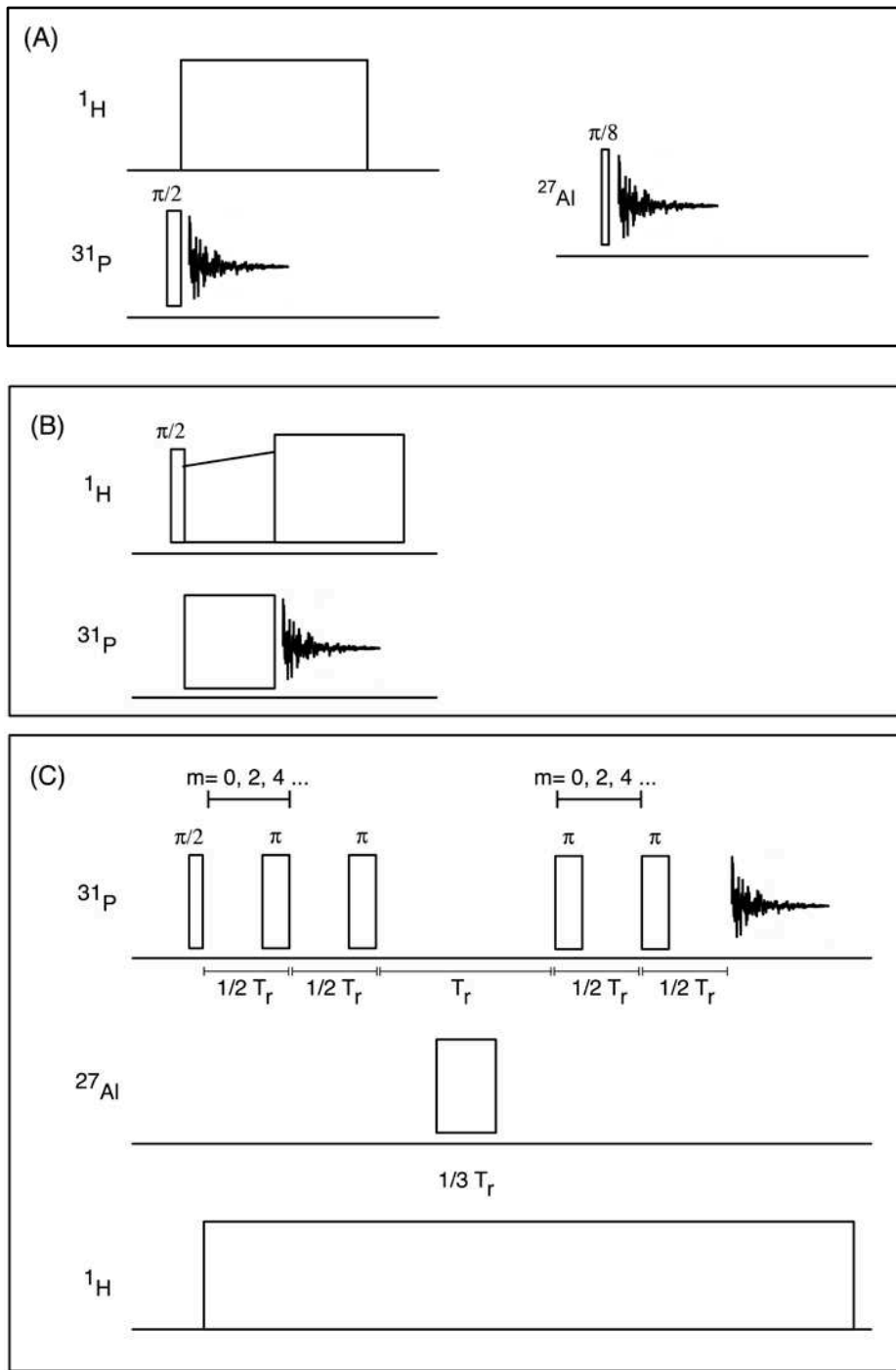


Figure 1. The NMR pulse sequences used for (A) ^{27}Al and ^{31}P MAS, (B) $^{31}\text{P}\{^1\text{H}\}$ CP/MAS, and (C) $^{31}\text{P}/^{27}\text{Al}$ REAPDOR experiments.

3. Results and Discussion

3.1. X-ray diffractometry (XRD)

Figure 2 displays the diffractograms for all samples evaluated. Well-defined and intense reflections of the crystalline calcium aluminate clinker phases are observed in the diffractogram of the anhydrous CAC (Figure 2A), including monocalcium aluminate (CaAl_2O_4 , pattern diffraction file (PDF) #01-070-0134), calcium titanate (CaTiO_3 , PDF #01-075-2100) and gehlenite ($\text{Ca}_2\text{Al}_2\text{SiO}_7$, PDF #00-035-0755). After 7 days of hydration of the CAC (Figure 2a), formation of both metastable CAH_{10} ($\text{CaO}\cdot\text{Al}_2\text{O}_3\cdot 10\text{H}_2\text{O}$, PDF #00-012-0408), and C_2AH_8 ($2\text{CaO}\cdot\text{Al}_2\text{O}_3\cdot 8\text{H}_2\text{O}$, PDF #00-045-0564), and stable hydrate phases including hydrogarnet C_3AH_6 ($3\text{CaO}\cdot\text{Al}_2\text{O}_3\cdot 6\text{H}_2\text{O}$, PDF #00-024-0217) and gibbsite ($\text{Al}(\text{OH})_3$, PDF #00-012-0401), is observed. At extended times of curing (180 days) (Figure 2A), the characteristic low-angle reflections of the metastable CAH_{10} ($\sim 12^\circ 2\theta$) and C_2AH_8 ($\sim 7^\circ 2\theta$) are not identified, and instead a significant increase in the intensity of the reflections assigned to the stable hydrates C_3AH_6 and AH_3 is observed. This suggests that the metastable phases have completely dissolved and re-precipitated as cubic hydrates within 180 days of curing. No significant changes in the intensity of the gehlenite and calcium titanate reflections are detected between 7 and 180 days of curing, indicating the low reactivity of these components upon hydration.

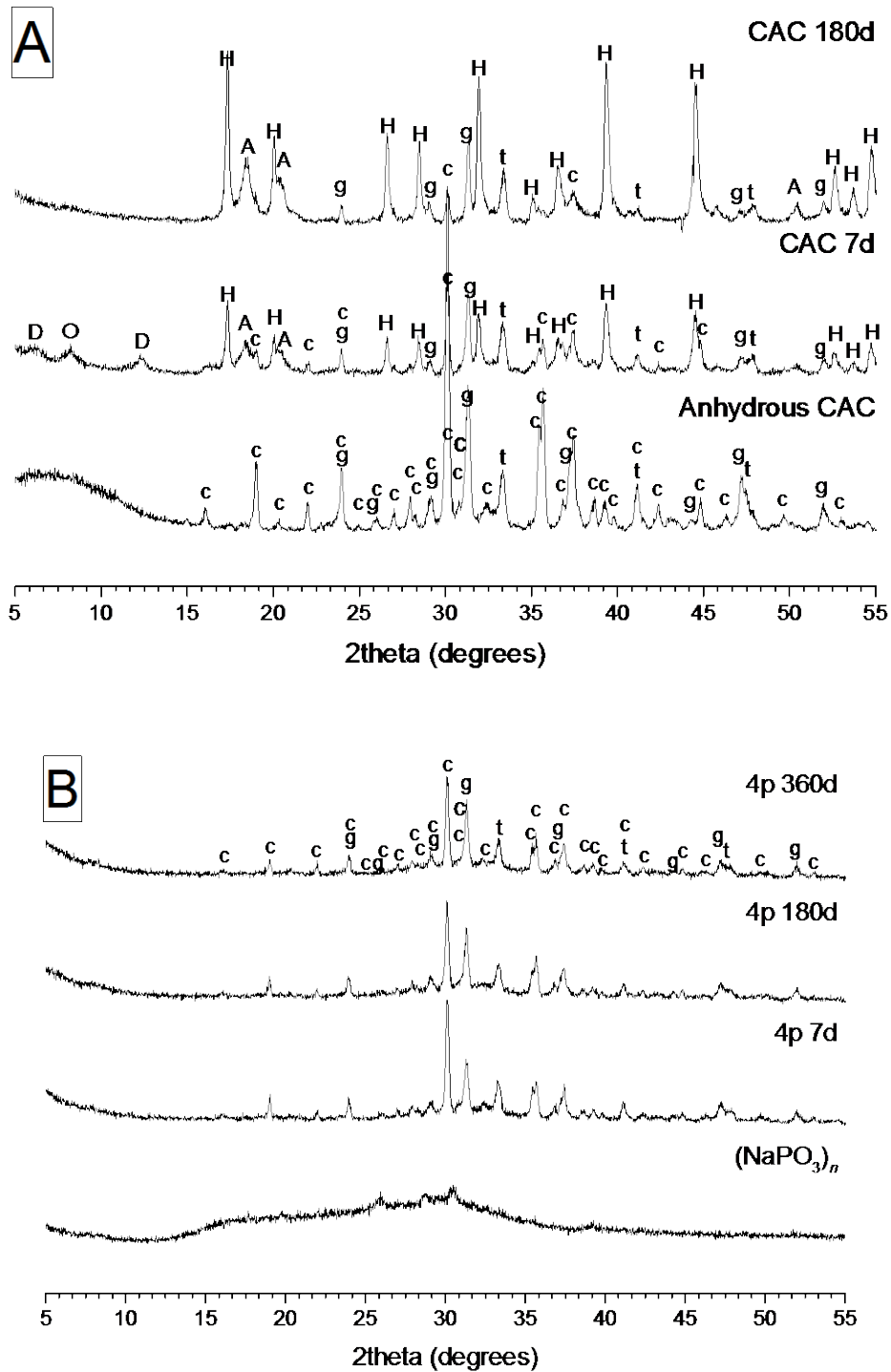


Figure 2. X-ray diffractograms of (A) CAC clinker and neat CAC samples at 7 and 180 days of curing, and (B) the polyphosphate modified CAC formulation (denoted 4p) after 7, 180 and 360 days of curing. Letters indicate phases identified, lowercase for

clinker phases monocalcium aluminate (c), gehlenite (g) and calcium titanate (t), and capitals for hydration products CAH₁₀ (D), C₂AH₈ (O), C₃AH₆ (H) and gibbsite (AH₃, A)

The diffractograms of the phosphate-modified CAC (Figure 2B) show no reflections for either the conventional hydrate products observed in hydrated CAC (Figure 2A) or any crystalline phases other than the anhydrous clinker phases, whose intensity reduces only slightly as a function of curing time. The only new feature observed is a broad diffuse scattering peak, centred at 30° 2θ, in all the polyphosphate modified samples, indicating that the precipitation of a phase with limited long-range order is occurring. The phosphate modification is altering the hydration pathway, avoiding conventional CAC hydrate precipitation and mitigating any potential issues surrounding conversion throughout the curing period considered in this study.

3.2. Thermogravimetry

The mass loss of CAC samples as a function of the sample temperature is shown in Figure 3, along with the data for the CAC clinker and the sodium polyphosphate, which are largely featureless and demonstrate that only the hydrate products contribute to the mass loss of the binders. The conventional CAC hydrates exhibit characteristic weight losses during heating as a result of dehydration reactions. The unmodified CAC sample hydrated for 7 days shows two regions of weight loss. The lower temperature exhibits a primary weight loss at 90°C with a secondary shoulder at 132°C, which indicate the presence of CAH₁₀ and C₂AH₈ respectively [35], consistent with the phases observed by XRD. A relatively wide range of dehydration temperatures are reported for these phases in the literature [36], however the sequence in which these phases dehydrate remains the same [35]. The gel phase present also dehydrates over a broad temperature range, partially overlapping with the dehydration of the CAH₁₀, which further

complicates the peak assignment [1]. The composition of this gel phase even in the unmodified CAC system is not fully understood, as it remains unclear whether this phase is a hydrated alumina gel (AH_n) [27,37] or a calcium aluminium hydrate (C-A-H) type gel [35,38,39].

Mass losses at higher temperatures are associated with the loss of structural water from the more thermodynamically favourable hydrates. Peaks for the dehydration of gibbsite [40] and C_3AH_6 [39], in the ranges 275–300°C and 300–315°C respectively, are observed in the data for the unmodified CAC. In the CAC sample cured for 180 days, weight losses corresponding to dehydration/decomposition of the hexagonal metastable phases are not identified, and instead the peaks corresponding to dehydration of AH_3 and C_3AH_6 are considerably more intense compared with those observed in specimens cured for 7 days. This indicates that the conversion of CAH_{10} and C_2AH_8 is essentially complete after 180 days of curing, in agreement with the diffraction data discussed in section 3.1. The residual mass loss in the low temperature range (below 200°C) for the 180 day cured sample can be assigned to the alumina-rich gel phase produced as a by-product of conversion, as discussed above.

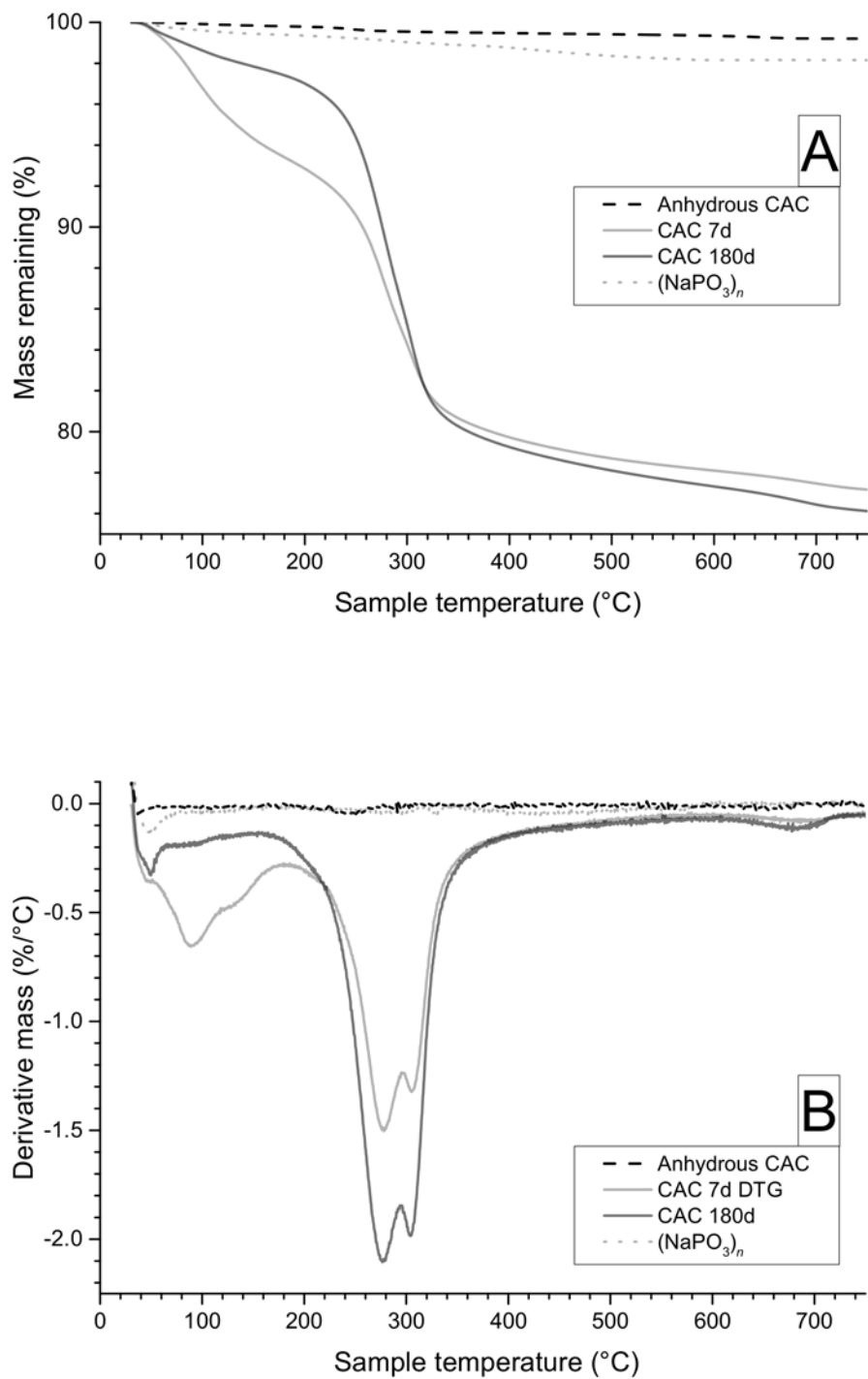


Figure 3 (A) Thermograms and (B) derivative thermograms of sodium polyphosphate, anhydrous CAC clinker, and CAC samples hydrated for 7 and 180 days.

The thermograms for the phosphate-modified CAC samples (Figure 4), show considerably different behaviour from the unmodified CAC samples (Figure 3). These samples exhibit three main weight losses, at ~90, 230 and 280°C, with broad peaks in the derivative curves consistent with non-crystalline water environments [38]. This is in agreement with the XRD results (Figure 2B) which did not show the formation of any crystalline hydrates in phosphate-modified CAC. Weight losses below 100°C generally indicate the dehydration of phases with loosely-bound water, and the evaporation of free water. In the case of the phosphate-modified CAC the largest weight loss, 90°C, may be attributed to the dehydration of the amorphous phase(s) forming in these systems, as indicated by the diffuse reflection in the XRD data (Figure 2B).

The weight loss at higher temperature (centred at ~280°C) is assigned to dehydroxylation of poorly crystalline gibbsite (AH_3), as in the unmodified CAC sample. The broad temperature range over which this weight loss takes place suggests low crystallinity, which is why this phase was not detected by XRD. Regarding the intermediate temperature weight loss (centered at ~230°C), Guirado et al. [38] identified that dehydration of CAH_{10} occurs in several stages, including a mass loss at 225°C associated with the dehydration of the amorphous portion (denoted CAH_y by those authors). It is possible that the mass loss observed in this temperature range in the phosphate-modified CAC may, analogously to that described by Guirado et al. [38], result from an initially disordered aluminate phase. An extended curing period does not seem to affect the phase assemblage of the material according to either XRD or thermogravimetry, but there is an increase in the intensity of the mass loss attributed to AH_3 between 7 and 180 days

curing, and a significant increase in mass loss in the region assigned to the amorphous gel type phase between 180 and 360 days curing, in Figure 4.

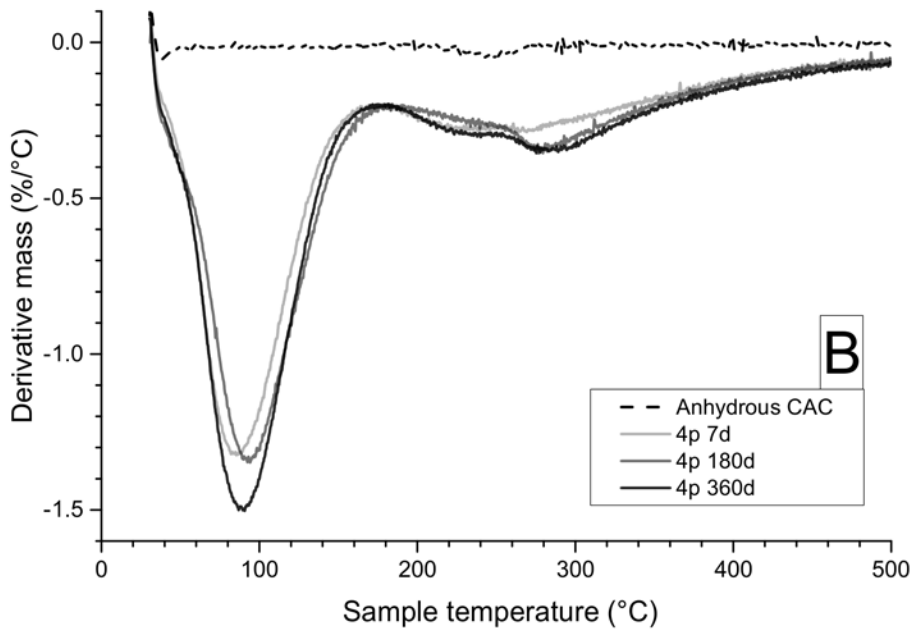
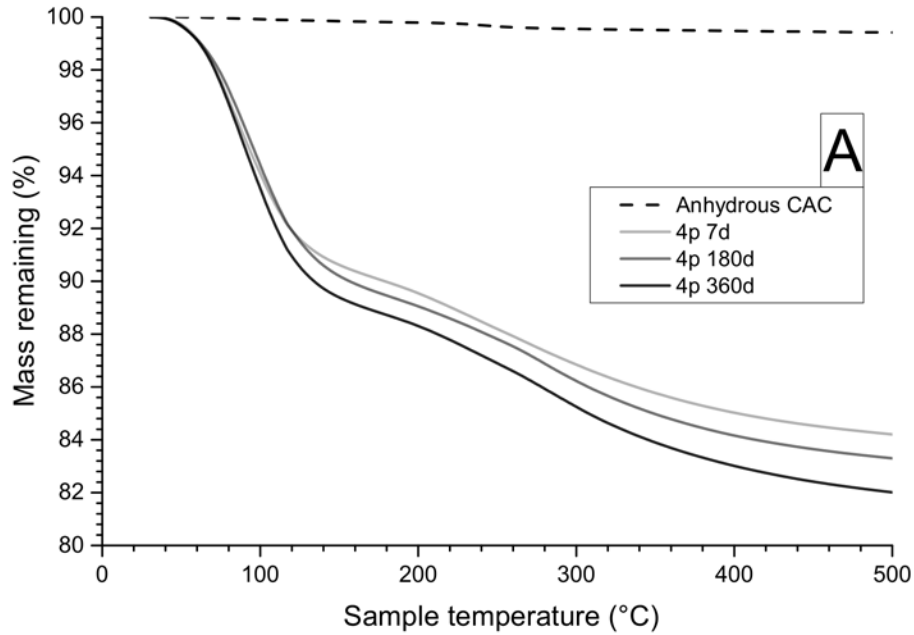


Figure 4 (A) Thermograms and (B) derivative thermograms for anhydrous CAC clinker and polyphosphate modified CAC samples (4p) hydrated for 7, 180 and 360 days.

3.3. Solid-state NMR spectroscopy

3.3.1. ^{27}Al MAS NMR

^{27}Al MAS NMR spectra of anhydrous CAC clinker and hydrated samples are shown in Figure 5A. ^{27}Al MAS NMR spectra typically show three distinct aluminium coordination environments (Al^{IV} , Al^{V} and Al^{VI}) which are located at chemical shifts between 52 to 80 ppm, 30 to 40 ppm, and -10 to 20 ppm, respectively [27,29]. The spectrum of the anhydrous CAC clinker in Figure 5A is dominated by a large resonance at 78 ppm, due to the tetrahedral aluminium in the CA present in the clinker [28], in addition to a very small response at 9 ppm indicative of the partial hydration of the materials during storage, consistent with the ~1% mass loss observed in the clinker by thermogravimetry, Figure 3.

The hydrated CAC samples in Figure 5A show reduced resonances in the Al^{IV} region as a result of the dissolution of clinker phases during hydration, and an increase in the Al^{VI} region as a result of precipitation of hexagonal and cubic hydrate phases. With increasing curing duration, the resonances of tetrahedral aluminium become less intense, as hydration nears completion at 180 days. A considerable change in the line shape in the Al^{VI} region is also observed between 7 and 180 days of curing as a result of the conversion of metastable CAH_{10} and C_2AH_8 to stable C_3AH_6 and AH_3 . The resonances at 8 (shoulder) and 12 ppm are consistent with the presence of AH_3 and C_3AH_6 respectively [41], consistent with the phases identified by X-ray diffraction (Figure 2) and thermogravimetry (Figure 3).

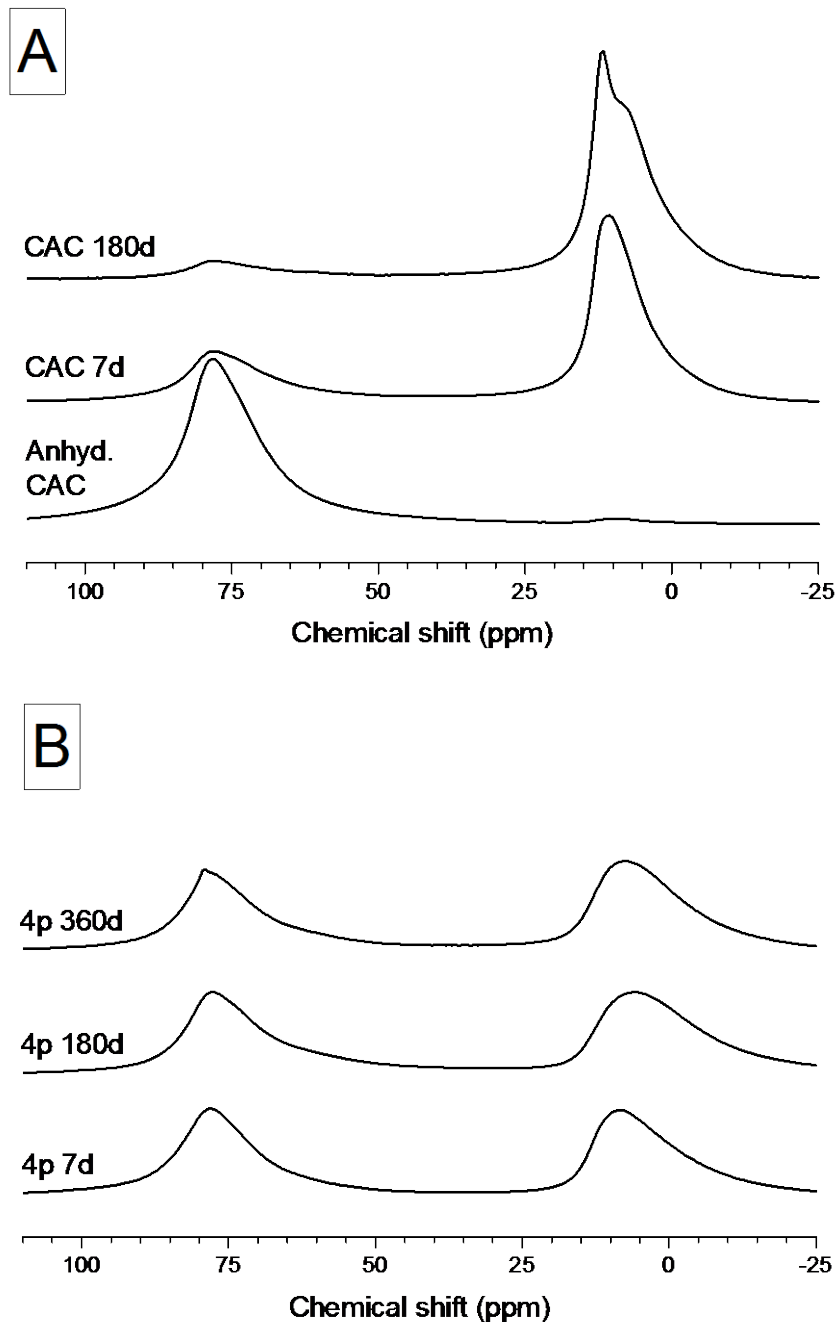


Figure 5. ^{27}Al MAS NMR spectra for (A) anhydrous CAC and CAC hydrated for 7 and 180 days, and (B) polyphosphate modified CAC samples (4p) hydrated for 7, 180 and 360 days.

Phosphate modified CAC samples (Figure 5B), exhibit spectra which are considerably different from those obtained for unmodified CAC samples. Resonances in regions associated with both

Al^{IV} and Al^{VI} coordinated environments are present. With increasing curing duration, the diffraction data indicate a marginally higher extent of dissolution of clinker phases in the tetrahedral region of the ²⁷Al MAS NMR spectra. There is also a slight change in the lineshape in this region, particularly at 360 days, indicating that this band may not be attributed solely to Al environments present in the remaining unreacted CAC clinker, and may also include contributions from a secondary Al^{IV}-containing phase forming in these systems.

The line shape and intensity of the two main bands identified in both the Al^{IV} and Al^{VI} regions of the spectra in Figure 5B seem to be similar after 7 days of curing; however, with increasing curing duration there is a small increase in the Al^{VI} band. The upfield peak for phosphate modified samples at all curing periods exhibited large peak widths (FWHMs of 16.3, 19.4, 17.5 ppm for 7, 180 and 360 day cured samples respectively) that could be assigned to either one phase with limited long range order, or the combination of a number of distinct contributions. This resonance is largely attributed to the presence of the gibbsite identified by thermogravimetry (Figure 4), although contributions from C-A-H or C-A-P-H gel may not be discounted as these could also hold aluminium in octahedral co-ordination. The formation of such a gel is also supported by thermogravimetry (peak at 225°C in Figure 4), considering its very low degree of long range order. However the precise identification of this gel necessitates the use of the phosphorus nucleus as a structural probe, and also the application of more advanced NMR techniques, as discussed below.

3.3.2. ³¹P MAS and ³¹P{¹H} CP/MAS NMR

Cross polarisation (CP) NMR experiments are a powerful probe of interatomic correlations, bringing added dependence upon proximity between two specific nuclei [42]. Here, the application of $^{31}\text{P}\{^1\text{H}\}$ CP/MAS NMR provides the possibility to establish whether phosphate environments are related to hydrogen atoms, which is essential in accurately characterising the gel phase present in the phosphate-modified CAC binder. The MAS spectrum of the polyphosphate precursor, Figure 6A, shows three broad responses at 1, -7 and -20 ppm, attributed to Q^0 , Q^1 and Q^2 phosphate structural units respectively [43,44], and the CP/MAS spectrum, Figure 6B, shows several sharp resonances corresponding to well-defined hydrous phosphate environments. The dissolution of the phosphate prior to blending with the CAC then results in a reduction of the Q^2 units as a result of hydrolysis, and this site is less evident in the binder products. The ^{31}P MAS and $^{31}\text{P}\{^1\text{H}\}$ CP/MAS spectra, Figure 6 (A) and (B), show very little change in the coordination environment of the phosphorus as a function of curing duration in the phosphate-modified CAC samples, corresponding to limited differences in the connectivity of the phosphate units and/or the electronegativity of next-nearest-neighbours [43].

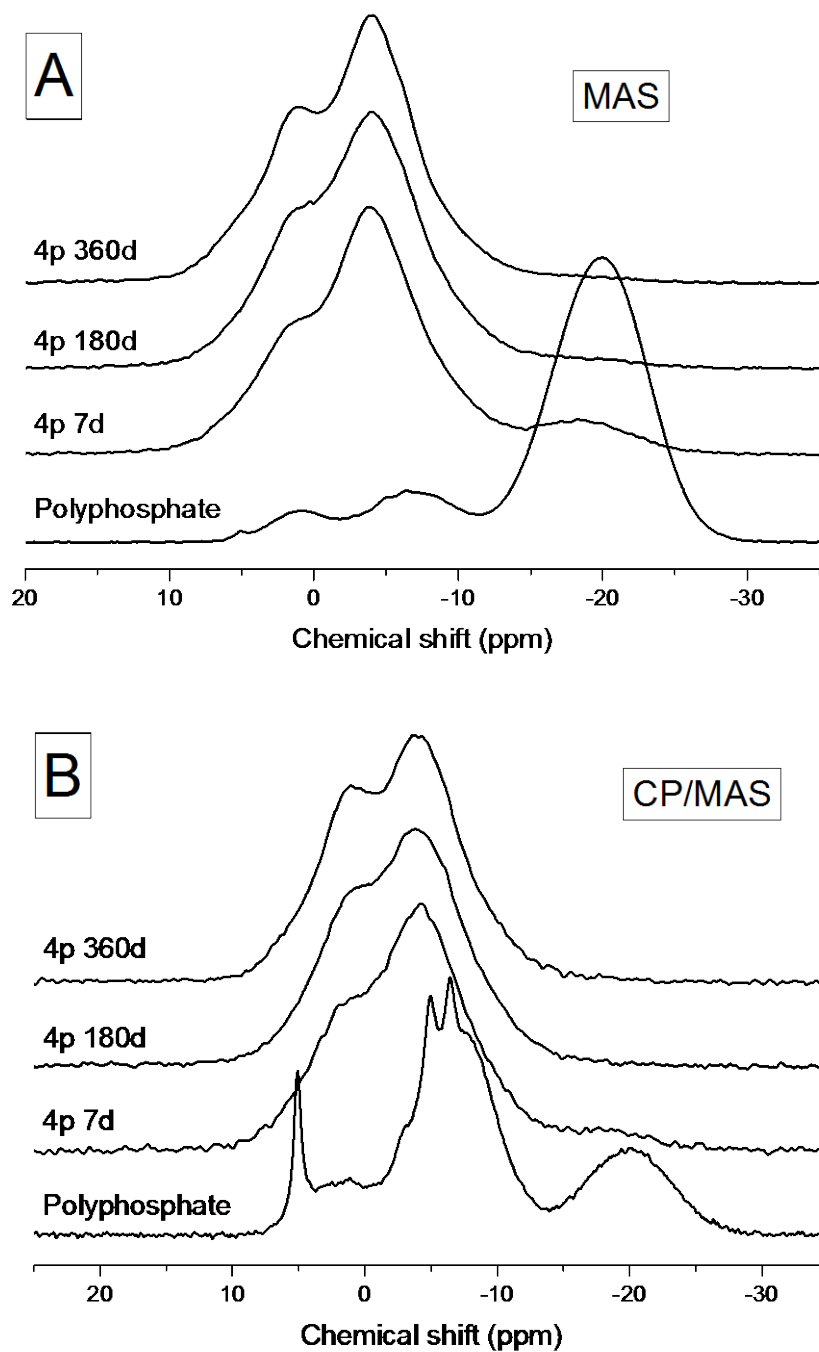


Figure 6 (a) ^{31}P MAS NMR spectra and (b) $^1\text{H}\{^{31}\text{P}\}$ cross polarisation MAS NMR spectra, for polyphosphate modified CAC samples and the sodium polyphosphate precursor.

In both sets of spectra (MAS and CP/MAS) for the hydration products of the phosphate-modified CAC, two broad main bands are identifiable at 1.1 (shoulder) and -4.1 ppm (main peak), indicating the presence of multiple relatively disordered hydrated phosphorus environments. The similar line shapes of the ^{31}P MAS and ^{31}P CP/MAS spectra indicate that all of the phosphorus environments in these samples are protonated to some extent, and thus the phosphorus environments are related to hydrate phases forming in these binders.

From the ^{31}P MAS NMR data alone, it is difficult to discern whether the resonances identified in these samples relate to calcium phosphate, aluminophosphate or C-A-P-H type phases. The resonance positions straddle the region for crystalline calcium phosphates [30,45-47] and the downfield limit reported for crystalline aluminophosphates [48,49], which are generally minerals holding aluminium in octahedral coordination [50], such as brazilianite $(\text{NaAl}_3(\text{PO}_4)_2(\text{OH})_4)$. Calcium aluminophosphates such as crandallite $\text{CaAl}_3(\text{PO}_4)_2(\text{OH})_5(\text{H}_2\text{O})$ have been reported to have intermediate ^{31}P chemical shifts (-1.81 [51] and -5.2 [49] ppm). Chemical shifts similar to those observed in Figure 6 (1.5 – 2.0 ppm depending on the Na/P ratio) have been reported [52] for sodium phosphate glasses with assignment to Q^1 environments. In studies of Ca-free sodium aluminophosphate glasses, Zhang and Eckert [53] reported ^{31}P chemical shifts of ~1.6 and -4.6 ppm, which they also assigned to Q^1 units with 0 and 1 bonded aluminium units respectively, in agreement with the results of Lang et al. [54].

The formation of aluminophosphate complexes as a result of phosphate interaction with aluminium oxides and hydroxides has been reported by a number of investigators [55-57]; particularly, corundum was reported [57] to form inner sphere surface complexes and surface

precipitates with phosphates. The surface complexes resonate at far more negative chemical shifts, < -11 ppm, than the sites identified here, but the chemical shifts at which the resonances occur for the phosphate modified CAC samples lie within the region identified as characteristic for inner sphere surface complexes [57]. So, the presence of such environments within the materials studied here would be in good agreement with these data. Investigations by Van Emmerik et al. [55] into phosphate sorption onto gibbsite also reported the formation of a number of different aluminium-containing phosphate environments, with inner sphere complexes dominating at pH 8, which is within 1-2 pH units of conditions in the modified CAC systems studied here. Kim and Kirkpatrick [50], examining phosphate adsorption onto aluminium oxyhydroxide, also identified surface adsorbed phosphate in inner-sphere complexes whose abundance increased with increasing pH, whilst the precipitation of crystalline aluminophosphates decreased. The formation of such complexes here would result in a diffusion barrier forming around the unreacted cement particles, inhibiting or significantly retarding further cement clinker hydration as well as consuming water of hydration, consistent with the reduced degree of reaction identified in the phosphate modified CACs by X-ray diffraction (Figure 2) compared with unmodified CACs.

3.3.3. $^{31}\text{P}/^{27}\text{Al}$ REAPDOR NMR

Further quantitative structural information can be obtained from REAPDOR (Rotational Echo Adiabatic Passage Double Resonance) analysis. Here, this experiment has been used to measure the dipolar coupling of the phosphorus and aluminium, which is proportional to $\gamma_P\gamma_{Al}/r^3$ (where γ_P and γ_{Al} are the gyromagnetic ratios of the two nuclei investigated, and r is the internuclear separation distance), and thus for the case of an isolated spin pair it is possible to calculate the

internuclear distance. Measurements are made as a function of dipolar evolution time, with and without the aluminium adiabatic dephasing pulse (see Figure 1) [58]. Signal intensities, S and S_0 , respectively, from these measurements are used to calculate the REAPDOR fraction: $\Delta S = (S_0 - S)/S_0$. REAPDOR experiments are very similar to the more common REDOR (rotational-echo double resonance) pulse schemes, but are more suitable to improve spin transitions of quadrupolar secondary nuclei [59].

The REAPDOR fraction ΔS was plotted against the dipolar evolution time, as shown in Figure 7. Each dataset is fitted with a universal REAPDOR equation, Eq. 1, for spin-1/2 and spin-5/2 nuclei, following Goldbourn et al. [58]. The universal fitting curve is a function of λ , $\lambda = (2m+2)T_r D$, where m is the number of rotor cycles, T_r the rotor period and D the dipolar coupling.

$$S_{\frac{1}{2}}^{REAP} c(\lambda) = 0.63(1 - e^{-(3.0\lambda)^2}) + 0.2(1 - e^{-(0.7\lambda)^2}) \quad (1)$$

The fitting of the REAPDOR data collected for phosphate modified CACs, obtaining r values by fitting λ in Eq.(1), yielded Al-P internuclear distances of 3.0 and 3.6 Å for the -4.1 and 1.1 ppm peaks respectively. It is noted that the universal curve is specifically defined for an isolated spin pair, and hence is at best an approximation to the exact bond lengths for bidentate structures such as the Q^2 environment identified here, where multiple interactions complicate the dipolar coupling. On purely geometric grounds, the Al-P interaction distances identified here seem rather short, and the bidentate nature of some of the complexes may be the reason for this. There is also not a clear aluminophosphate resonance in the ^{27}Al MAS NMR spectra in Figure 5. Nonetheless,

it is clear that the -4.1 ppm peak corresponds to a shorter Al-P interaction distance than the 1.1 ppm peak.

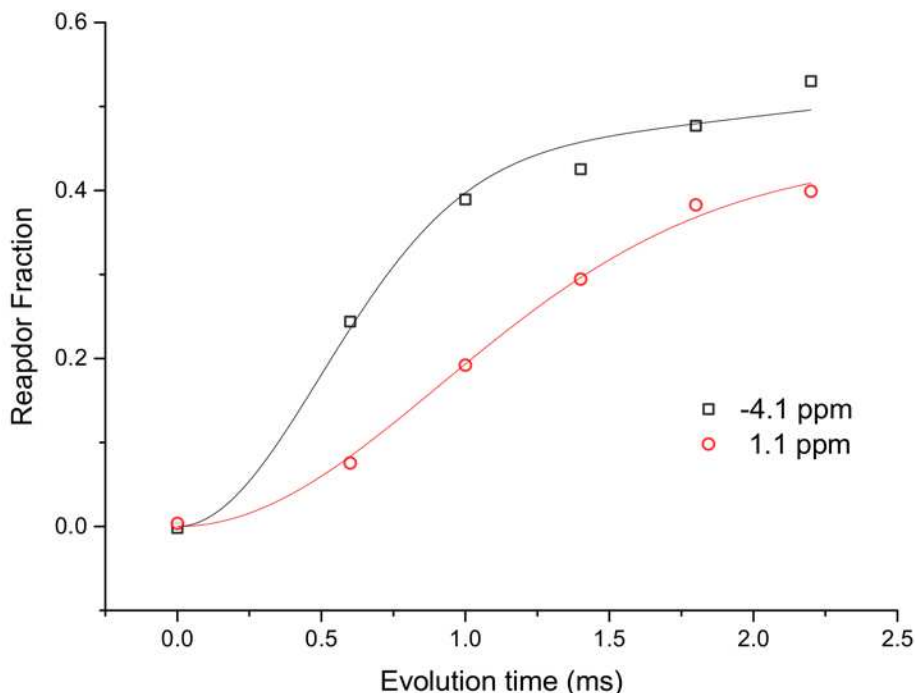


Figure 7. Peak-resolved dephasing curves for $^{31}\text{P}/^{27}\text{Al}$ REAPDOR NMR analysis of the polyphosphate-modified CAC sample cured for 360 days

At longer evolution times, longer-range interactions can contribute to the dephasing, resulting in a poorer fit with Eq. 1, hence the dipolar evolution time was limited to 2.2 ms. As a result of a convoluted signal, where some contributions are from environments without aluminium-phosphorus interactions, even at greater evolution periods some residual response is present in the spectra despite the adiabatic dephasing pulse on the secondary channel, and hence the REAPDOR fractions do not reach unity. To account for this residual response, Eq. 1 was modified by an empirically fitted scaling factor.

Investigations of the dipolar coupling between aluminium and phosphorus in the samples indicate a fair degree of intimacy between the two, as seen by the dephasing of the signal, and lead us to believe that previous explanations of the hydrate chemistry which did not consider alumino-phosphate phases do not describe this system fully. The resonant frequencies of the bands identified in the ^{31}P spectra, and the shielding effects of calcium and aluminium on chemical shift, suggest the possibility of a C-A-P-H phase with little long-range order. Due to the broad peak widths, the presence of a calcium orthophosphate as suggested by Sugama et al. [24] cannot be entirely discounted, but it appears much more likely that the majority of the phosphate sites in the disordered component are intimately intermixed with aluminate species rather than in a well-defined Al-free phosphate phase.

3.4. Compressive strength

The compressive strength development of the polyphosphate modified material, shown in Figure 8, indicates strengths of up to 31 MPa within the first 48 hours of curing. This early strength development is characteristic of reactive CAC materials and is one of the reasons for the addition of CAC to OPC based clinkers to adjust the setting behaviour. The considerable differences in the kinetics of reaction between early age 4p samples and those at longer curing periods, as seen in thermogravimetric data (section 3.2) and their respective NMR spectra (section 3.3), correlate well with the compressive strength data for these systems. The high initial strength of the phosphate-modified CAC is maintained; however, at seven days of hydration this seems to increase rapidly, followed by a steady increase continuing at least until 360 days, where a value

of 73 MPa is noted. This is in contrast to a similar high initial strength after 48 hours for the unmodified CAC which then rises to 58 MPa at 4 days, even though a larger fraction of CAC seem to be reacting at a given time of curing in this unmodified system.

In the unmodified CAC, the initial maximum in strength after 7 days of curing, with a fall in compressive strength thereafter, is attributed to the conversion process, whereby the dissolution of metastable phases and the precipitation of denser stable phases result in a considerable increase in the porosity of the material, reducing the mechanical integrity of the material. This supports the clear differences seen in the earlier characterisation of the CAC samples, between the samples cured for 7 days and those cured for 180 days.

The compressive strengths obtained in this study for 4p samples are in good agreement with those reported by Sugama et al. (30 MPa after 72 hours) [21], but lower than those obtained by Swift et al. (77 MPa after 72 hours) [8] for phosphate modified CAC. This difference in strength is attributed to the use of higher water/cement and phosphate/cement ratios in the present study, compared with those utilised by Swift et al. [8], which will significantly affect key parameters controlling the compressive strength development, such as degree of reaction and porosity of the system.

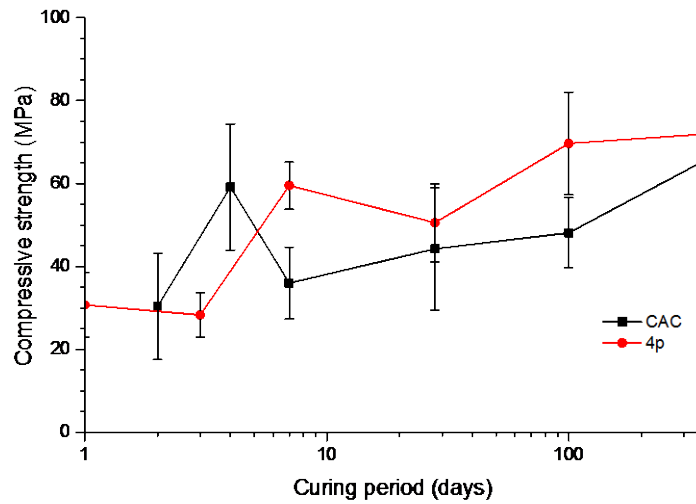


Figure 8. Compressive strength data for 4p samples at various ages, compared to unmodified CAC

The higher compressive strength developed by the phosphate modified CAC elucidates that, even though reduced degrees of CAC reaction might take place at a given age, the fact that the phosphate addition hinders the conversion process, along with the formation of a poorly crystalline secondary reaction product, has a positive effect in the long term mechanical performance of these materials.

4. Conclusions

The phosphate modification of calcium aluminate cement results in a significant deviation away from the conventional hydration behaviour of calcium aluminate cement. None of the conventional crystalline calcium aluminate hydrates were detected in phosphate-modified samples, either by XRD or by thermal analysis, during a curing period of one year. The alteration of the hydration pathway away from conventional crystalline phase precipitation, achieved

through phosphate modification, has thus been shown to be effective in avoiding the calcium aluminate hydrate conversion process, at least for the curing periods studied.

The understanding of the hydration mechanism and phase assemblage of phosphate modified CAC is challenging due to the difficulty in characterising the very poorly crystalline hydrates forming. The weight loss identified by thermogravimetry below 200°C is difficult to resolve, however it is likely that in the absence of any conventional crystalline hydrates precipitating, a calcium aluminate hydrate-based gel is forming in addition to the poorly crystalline gibbsite detected by the same method. The formation of phosphate complexes at phosphate-aluminium hydroxide interfaces is well established in the literature, and therefore, it is possible that a similar mechanism is resulting in the formation of phosphate complexes at the interface with the amorphous gibbsite.

The phosphate-modified CAC systems are also seen by REAPDOR NMR to contain considerable dipolar interactions between the aluminium and phosphorus, supporting the identification of phases with these elements intimately intermixed. The ³¹P MAS NMR spectra are consistent with the presence of calcium within these phases, and CP/MAS NMR shows that they are hydrous, resulting in the final identification of a disordered C-A-P-H type gel as being an important phase within these binders. These complex gels would be the primary reason for the deviation from conventional hydrate phase formation, and also the prevention of further hydration of the unreacted clinker particles at extended times of curing.

Acknowledgements

This work was funded by the Engineering and Physical Sciences Research Council (EPSRC).

Solid-state NMR spectra were obtained at the EPSRC UK National Solid-state NMR Service at Durham.

References

- [1] K.L. Scrivener, Calcium Aluminate Cements, in: *Advanced Concrete Technology*, J. Newman & B.S. Choo, eds., Elsevier, Oxford, 2003.
- [2] A. Macias, A. Kindness, F.P. Glasser, Corrosion behaviour of steel in high alumina cement mortar cured at 5, 25 and 55° C: chemical and physical factors, *J. Mater. Sci.* 31 (1996) 2279–2289.
- [3] M.C.G. Juenger, F. Winnefeld, J.L. Provis, J.H. Ideker, Advances in alternative cementitious binders, *Cem. Concr. Res.* 41 (2011) 1232–1243.
- [4] L. Kraft, L. Hermansson, Dimension Stable Binding Agent Systems for Dental Application, US Patent No. US6620232 B1, 2003.
- [5] J. Bensted, P. Barnes, eds., *Structure and Performance of Cements*, 2nd ed., Spon Press, London, 2002.

- [6] P.C. Hewlett, ed., *Lea's Chemistry of Cement and Concrete*, 4th ed., Butterworth-Heinemann, Oxford, 2003.
- [7] T. Sugama, *Advanced Cements for Geothermal Wells*, BNL-77901-2007-IR, Brookhaven National Laboratory, New York, 2006.
- [8] P.D. Swift, H. Kinoshita, N.C. Collier, C.A. Utton, Phosphate modified calcium aluminate cement for radioactive waste encapsulation, *Adv. Appl. Ceram.* 112 (2013) 1–8.
- [9] H. Kinoshita, P.D. Swift, C.A. Utton, B. Carro-Mateo, G. Marchand, N.C. Collier, et al., Corrosion of aluminium metal in OPC- and CAC-based cement matrices, *Cem. Concr. Res.* 50 (2013) 11–18.
- [10] N.B. Milestone, Reactions in cement encapsulated nuclear wastes: need for toolbox of different cement types, *Adv. Appl. Ceram.* 44 (2006) 3–10.
- [11] M.I. Ojovan, W.E. Lee, *An Introduction to Nuclear Waste Immobilisation*, Elsevier, Oxford, 2005.
- [12] J.M. Fernández, I. Navarro-Blasco, A. Duran, R. Sirera, J.I. Alvarez, Treatment of toxic metal aqueous solutions: encapsulation in a phosphate-calcium aluminate matrix, *J. Environ. Manag.* 140 (2014) 1–13.
- [13] A.M. Neville, History of high-alumina cement. Part 1: Problems and the Stone report, *Proc. ICE-Eng. Hist. Herit.* 162 (2009) 81–91.

- [14] A. Fernández-Jiménez, T. Vázquez, Á. Palomo, Effect of sodium silicate on calcium aluminate cement hydration in highly alkaline media: A microstructural characterization, *J. Am. Ceram. Soc.* 94 (2011) 1297–1303.
- [15] N.Y. Mostafa, Z.I. Zaki, O.H. Abd Elkader, Chemical activation of calcium aluminate cement composites cured at elevated temperature, *Cem. Concr. Compos.* 34 (2012) 1187–1193.
- [16] A. Hidalgo, J.L. García, M. Cruz Alonso, L. Fernández, C. Andrade, Microstructure development in mixes of calcium aluminate cement with silica fume or fly ash, *J. Therm. Anal. Calorim.* 96 (2009) 335–345.
- [17] L. Fernández-Carrasco, E. Vázquez, Reactions of fly ash with calcium aluminate cement and calcium sulphate, *Fuel.* 88 (2009) 1533–1538.
- [18] A.J. Majumdar, B. Singh, Properties of some blended high-alumina cements, *Cem. Concr. Res.* 22 (1992) 1101–1114.
- [19] T. Sugama, M. Allan, J.M. Hill, Calcium phosphate cements prepared by acid–base reaction, *J. Am. Ceram. Soc.* 75 (1992) 2076–2087.
- [20] T. Sugama, N.R. Carciello, Sodium phosphate-derived calcium phosphate cements, *Cem. Concr. Res.* 25 (1995) 91–101.
- [21] T. Sugama, N.R. Carciello, Strength development in phosphate-bonded calcium aluminate cements, *J. Am. Ceram. Soc.* 74 (1991) 1023–30.

- [22] W. Ma, P.W. Brown, Mechanical behavior and microstructural development in phosphate modified high alumina cement, *Cem. Concr. Res.* 22 (1992) 1192–1200.
- [23] T. Sugama, M. Taylor, Interfacial and mechanical behavior of fiber-reinforced calcium phosphate cement composites, *Cem. Concr. Compos.* 16 (1994) 93–106.
- [24] T. Sugama, L. Weber, L.E. Brothers, Resistance of sodium polyphosphate-modified fly ash/calcium aluminate blend cements to hot H₂SO₄ solution, *Cem. Concr. Res.* 29 (1999) 1969–1976.
- [25] W. Ma, P.W. Brown, Hydration of sodium phosphate-modified high alumina cement, *J. Mater. Res.* 4801 (1994).
- [26] H.F.W. Taylor, *Cement Chemistry*, Academic Press, London, 1990.
- [27] J. Skibsted, E. Henderson, H.J. Jakobsen, Characterization of calcium aluminate phases in cements by ²⁷Al MAS NMR spectroscopy, *Inorg. Chem.* 32 (1993) 1013–1027.
- [28] X. Cong, R.J. Kirkpatrick, Hydration of calcium aluminate cements: A solid-state ²⁷Al NMR study, *J. Am. Ceram. Soc.* 76 (1993) 409–16.
- [29] D. Müller, W. Gessner, H.-J. Behrens, G. Scheler, Determination of the aluminium coordination in aluminium-oxygen compounds by solid-state high-resolution ²⁷Al NMR, *Chem. Phys. Lett.* 79 (1981) 59–62.

- [30] A.P. Legrand, H. Sfihi, N. Lequeux, J. Lemaître, ^{31}P solid-state NMR study of the chemical setting process of a dual-paste injectable brushite cements., *J. Biomed. Mater. Res. B. Appl. Biomater.* 91 (2009) 46–54.
- [31] A. Stamboulis, S. Matsuya, R.G. Hill, R. V Law, K. Udoh, M. Nakagawa, et al., MAS-NMR spectroscopy studies in the setting reaction of glass ionomer cements., *J. Dent.* 34 (2006) 574–81.
- [32] S.L. Poulsen, H.J. Jakobsen, J. Skibsted, Incorporation of phosphorus guest ions in the calcium silicate phases of Portland cement from ^{31}P MAS NMR spectroscopy., *Inorg. Chem.* 49 (2010) 5522–9.
- [33] F. Rashchi, J.A. Finch, Polyphosphates: a review their chemistry and application with particular reference to mineral processing, *Miner. Eng.* 13 (2000) 1019–1035.
- [34] M.A. Chavda, H. Kinoshita, J.L. Provis, Phosphate modification of calcium aluminate cement to enhance stability for immobilisation of metallic wastes, *Adv. Appl. Ceram.* 113 (2014) 453-459.
- [35] S.M. Bushnell-Watson, J.H. Sharp, The application of thermal analysis to the hydration and conversion reactions of calcium aluminate cements, *Mater. Constr.* 42 (1992) 13–32.
- [36] N. Ukrainczyk, T. Matusinović, S. Kurajica, B. Zimmermann, J. Sipusic, Dehydration of a layered double hydroxide - C_2AH_8 , *Thermochim. Acta.* 464 (2007) 7–15.
- [37] K. Fujii, W. Kondo, H. Ueno, Kinetics of hydration of monocalcium aluminate, *J. Am. Ceram. Soc.* 64 (1986) 361–364.

- [38] F. Guirado, S. Galí, J.S. Chinchón, Thermal decomposition of hydrated alumina cement (CAH₁₀), *Cem. Concr. Res.* 28 (1998) 381–390.
- [39] V.S. Ramachandran, R.M. Paroli, J.J. Beaudoin, A.H. Delgado, *Handbook of Thermal Analysis of Construction Materials*, Noyes Publications, New York, 2002.
- [40] V. Balek, J. Šubrt, J. Rouquerol, P. Llewellyn, V. Zelenák, I.M. Bountsewa, et al., Emanation thermal analysis study of synthetic gibbsite, *J. Therm. Anal. Calorim.* 71 (2003) 773–782.
- [41] D. Müller, A. Rettel, W. Gessner, G. Scheler, An application of solid-state magic-angle spinning ²⁷Al NMR to the study of cement hydration, *J. Magn. Reson.* 57 (1984) 152–156.
- [42] K.J.D. MacKenzie, M.E. Smith, *Multinuclear Solid State NMR of Inorganic Materials*, Pergamon, Oxford, 2002.
- [43] G.L. Turner, R.J. Kirkpatrick, S.H. Risbud, E. Oldfield, Multinuclear magic-angle sample-spinning nuclear magnetic resonance spectroscopic studies of crystalline and amorphous ceramic materials, *Am. Ceram. Soc. Bull.* 66 (1987) 656–663.
- [44] R.K. Brow, R.J. Kirkpatrick, G.L. Turner, Nature of alumina in phosphate glass: II, Structure of sodium aluminophosphate glass, *J. Am. Ceram. Soc.* 76 (1993) 919–928.
- [45] Z. He, C.W. Honeycutt, B. Xing, R.W. McDowell, P.J. Pellechia, T. Zhang, Solid-state Fourier transform infrared and ³¹P nuclear magnetic resonance spectral features of phosphate compounds, *Soil Sci.* 172 (2007) 501–15.

- [46] J.L. Miquel, L. Facchini, A.P. Legrand, C. Rey, J. Lemaître, Solid state NMR to study calcium phosphate ceramics, *Colloids Surf.* 45 (1990) 427–433.
- [47] F. Pourpoint, C. Gervais, L. Bonhomme-Coury, T. Azais, C. Coelho, F. Mauri, et al., Calcium phosphates and hydroxyapatite: Solid-state NMR experiments and first-principles calculations, *Appl. Magn. Reson.* 32 (2007) 435–457.
- [48] M.A. Fedotov, I.L. Mudrakovskii, V.M. Mastikhin, V.P. Shmachkova, N.S. Kotsarenko, Dependence of the ^{27}Al and ^{31}P NMR chemical shifts in alumophosphates on the composition of the second coordination sphere, *Bull. Acad. Sci. USSR.* 36 (1987) 2169–71.
- [49] W.F. Bleam, P.E. Pfeffer, J.S. Frye, ^{31}P solid-state nuclear magnetic resonance spectroscopy of aluminum phosphate minerals, *Phys. Chem. Miner.* 16 (1989) 455–464.
- [50] Y. Kim, R.J. Kirkpatrick, An investigation of phosphate adsorbed on aluminium oxyhydroxide and oxide phases by nuclear magnetic resonance, *Eur. J. Soil Sci.* 55 (2004) 243–251.
- [51] R.J.P. Williams, R.G.F. Giles, A.M. Posner, Solid state phosphorus NMR spectroscopy of minerals and soils, *J. Chem. Soc. Chem. Commun.* (1981) 1051–2.
- [52] R.K. Brow, R.J. Kirkpatrick, G.L. Turner, Local structure of $x\text{Al}_2\text{O}_3 \cdot (1-x)\text{NaPO}_3$ glasses: an NMR and XPS study, *J. Am. Ceram. Soc.* 73 (1990) 2293–300.

- [53] L. Zhang, H. Eckert, Short- and medium-range order in sodium aluminophosphate glasses: new insights from high-resolution dipolar solid-state NMR spectroscopy., *J. Phys. Chem. B.* 110 (2006) 8946–58.
- [54] D.P. Lang, T.M. Alam, D.N. Bencoe, Solid-state $^{31}\text{P}/^{27}\text{Al}$ and $^{31}\text{P}/^{23}\text{Na}$ TRAPDOR NMR investigations of the phosphorus environments in sodium aluminophosphate glasses, *Chem. Mater.* 13 (2001) 420–428.
- [55] T.J. Van Emmerik, D.E. Sandström, O.N. Antzutkin, M.J. Angove, B.B. Johnson, ^{31}P solid-state nuclear magnetic resonance study of the sorption of phosphate onto gibbsite and kaolinite, *Langmuir.* 23 (2007) 3205–13.
- [56] W. Li, J. Feng, K.D. Kwon, J.D. Kubicki, B.L. Phillips, Surface speciation of phosphate on boehmite ($\gamma\text{-AlOOH}$) determined from NMR spectroscopy, *Langmuir.* 26 (2010) 4753–61.
- [57] W. Li, A.-M. Pierre-Louis, K.D. Kwon, J.D. Kubicki, D.R. Strongin, B.L. Phillips, Molecular level investigations of phosphate sorption on corundum ($\alpha\text{-Al}_2\text{O}_3$) by ^{31}P solid state NMR, ATR-FTIR and quantum chemical calculation, *Geochim. Cosmochim. Acta.* 107 (2013) 252–266.
- [58] A. Goldbourt, S. Vega, T. Gullion, A.J. Vega, Interatomic distance measurement in solid-state NMR between a spin-1/2 and a spin-5/2 using a universal REAPDOR curve., *J. Am. Chem. Soc.* 125 (2003) 11194–5.

Preprint version of accepted article. Please cite as:

*M.A. Chavda, S.A. Bernal, D.C. Apperley, H. Kinoshita, J.L. Provis. "Identification of the hydrate gel phases present in phosphate-modified calcium aluminate binders", *Cement and Concrete Research* 2015, 70:21-28.*

Official journal version is online at <http://dx.doi.org/10.1016/j.cemconres.2015.01.007>

- [59] E. Hughes, T. Gullion, A. Goldbourn, S. Vega, A.J. Vega, Internuclear distance determination of S=1, I=1/2 spin pairs using REAPDOR NMR, *J. Magn. Reson.* 156 (2002) 230–241.